minerals

MDPI

Article

Metallic Copper (Cu[0]) Obtained from Cu^{2+}-Rich Acidic Mine Waters by Two Different Reduction Methods: Crystallographic and Geochemical Aspects

Javier Sánchez-España [1,*], Andrey Ilin [2] and Iñaki Yusta [2]

[1] Mine Waste and Environmental Geochemistry Research Group, Department of Geological Resources (IGME-CSIC), Calera 1, Tres Cantos, 28760 Madrid, Spain
[2] Department of Geology, University of the Basque Country (UPV/EHU), Faculty of Science and Technology, Apdo. 644, 48080 Bilbao, Spain; andrey.ilin@ehu.eus (A.I.); i.yusta@ehu.eus (I.Y.)
* Correspondence: j.sanchez@igme.es

Abstract: The recovery of valuable metals from different types of wastes has become of prime strategic interest given the scarcity of primary critical raw materials at international scale. Implementation of new methods or refinement of classical techniques with modern technological advances is, therefore, an active research field. Mine wastes are of special interest because their high metal concentrations make them environmentally harmful and economically profitable at the same time. In this study, we evaluated two different methods of Cu recovery from extremely acidic mine waters seeping from wastes and abandoned mines in SW Spain. Through a series of different batch experiments, we compared the method efficiency and crystallographic properties of elemental copper (Cu[0]) obtained by reduction of Cu^{2+} ions by (1) chemical reduction using ascorbic acid at different environmental conditions of pH (1.50–3.95), temperature (25–80 °C) and ascorbic acid concentration (10 mM to 0.1 M), and (2) classical cementation method with scrap iron at pH 1.50 and 25 °C. Our study demonstrates that the precipitation of Cu[0] can take place at pH 3.95 and low AA concentrations (0.1 M), resulting in large (µm-scale), perfectly developed crystals of copper with pseudoprismatic to acicular habit after 24 h of aging, likely through formation of a transient compound consisting in Cu^{2+}-ascorbate and/or cuprite (Cu_2O) nanocolloids. Reduction experiments at higher AA concentrations (0.1 M) showed faster precipitation kinetics and resulted in high-purity (>98%) copper suspensions formed by subrounded nanoparticles. The AA method, however, yielded very low recovery rates (15–25%) because of the low pH values considered. The cementation method, which produced tree-like aggregates formed by sub-micron crystals arranged in different directions, proved to be much more efficient (>98% recovery) and cost-effective.

Keywords: copper; chemical reduction; acidic mine waters; secondary raw materials; metal recovery

Citation: Sánchez-España, J.; Ilin, A.; Yusta, I. Metallic Copper (Cu[0]) Obtained from Cu^{2+}-Rich Acidic Mine Waters by Two Different Reduction Methods: Crystallographic and Geochemical Aspects. *Minerals* **2022**, *12*, 322. https://doi.org/10.3390/min12030322

Academic Editors: Radoslaw Pomykala, Barbara Tora and Katerina Adam

Received: 31 January 2022
Accepted: 1 March 2022
Published: 4 March 2022

1. Introduction

Copper is of paramount importance in modern technology, being widely used in micro/nanoelectronics [1]. Copper nanoparticles and nanowires are also of major interest for their use in diverse fields, such as catalysis, optoelectronics, and liquid phase or gas sensors [2–4]. Copper nanoparticles are also used to produce conductive inks for electrodes of silicon crystal solar cells and in the printed electronic industry [5]. Other potential applications of copper nanoparticles aim to take advantage of their known antibacterial properties in the food or medical industry, or to produce lubricating substances for the fabrication of diverse composite materials [2]. Copper nanoparticles have been traditionally obtained by reduction of Cu^{2+} ions in solution, which does not require expensive equipment and allows the control of particle size and morphology through variation of certain parameters [2]. This method usually requires an alkaline pH to be efficient, since the electrode potential of AA is much lower at alkaline medium (+80 mV compared to

+166 mV at pH 4 [2]). At present, copper nanoparticles may be synthesized by different reduction methods using microwaves, as well as sonochemical, electrochemical, thermal, and chemical techniques, whereas copper nanowires are currently produced by different methods such as electrochemical deposition/electroplating (commonly the easiest and cheapest technique, and highly efficient at very acidic pH), pulsed laser deposition, or chemical vapor deposition [3,6–8]. In chemical reduction, the use of several reductants in early times, such as hydrazine or sodium hydrophosphate, which were seen to be either highly toxic (e.g., hydrazine) or technically inefficient (e.g., sodium hydrophosphate), has been progressively replaced by other reducing agents, such as ascorbic acid and other organic reductants such as glucose [2,3,5]. The antioxidant properties of AA (which prevent the resulting copper from undergoing oxidation in oxygenated environments) make this compound advantageous with respect to other reductants [3]. The control of size and morphology of Cu[0] and Cu_2O nanocrystals and nanostructures through the use of different organic and inorganic additives, with or without stabilizing agents, has also become a common practice in materials chemistry to produce nanomaterials with very specific conductive properties (e.g., superconductors) [9].

In the context of a high demand of raw materials for the modern industry and the implementation of circular economy concepts at global scale, the recovery of valuable and critical metals from mine wastes has become of growing interest [10]. Acidic mine waters seeping from mine wastes (e.g., tailings, waste piles) or abandoned mine portals or open pits, usually referred to as acid mine drainage (AMD), is among the major environmental problems of the metal and coal mining industry, due to its severe acidity and high concentration of sulfate and many toxic metals [11,12]. At the same time, however, these acidic liquors may contain valuable metals, such as Cu, Zn, Co, or Ni, at such high concentrations that can make them a resource of secondary raw materials more than a waste [13–15]. The acidic mine waters of the Iberian Pyrite Belt, in SW Spain, with AMD leachates exceeding concentrations of 440 ppm (mg/L) [16] and with pit lakes showing extreme contents up to 1350 mg/L Cu^{2+} [17–19], probably represent a paradigmatic case at international level. Although its benefit at industrial scale by modern techniques is still utopic, the recovery of copper by the classical cementation method using scrap iron was widely used in the region during the 19th and 20th centuries [20], being also applied at present in some AMD sites and pit lakes in other mining districts of the world [21].

Despite the plethora of studies on different methods of copper production from solutions of variable chemistry and origin, there is an apparent lack of studies comparing the efficiency of different methods potentially applicable to the recovery of copper from AMD, and both the structural/crystallographic properties of the obtained copper by reduction of Cu^{2+} ions, and the geochemical controls on Cu[0] crystallization, are still not sufficiently well known. Any Cu^{2+}-reduction method needs to be cost-effective and must provide a high-quality product in order to be profitable and implementable at industrial scale. In the present study, we aimed to evaluate the efficiency of Cu^{2+} reduction in Cu-rich, acidic mine waters by (1) chemical reduction using ascorbic acid (a widely known reducing agent in Cu synthesis studies), and (2) classical cementation method using scrap iron as reducing agent. Both methods were tested at low pH conditions (<4.0) under oxygenic atmosphere and without any stabilizer, since the main goal of our investigation was to evaluate possible on-site treatments in abandoned mines without the need of complex or expensive infrastructure. We were especially interested in contrasting the geometry and size of the copper particles and/or crystals formed by these two different methods, for which we used a combination of X-ray diffraction and scanning electron microscopy. Geochemical modeling based on solution chemistry was also used to evaluate the distribution and molar abundance of Cu aqueous species in solution and the saturation state of the acidic solutions with respect to elemental copper and other copper compounds. The practical implications are discussed.

2. Materials and Methods

2.1. Field Work and Sampling

Water samples (1 L each) were taken from three different locations in the province of Huelva (SW Spain), a region severely affected by acid mine drainage (AMD) pollution [16]. These acidic mine waters included a leachate from a big waste rock pile in the Riotinto mine (TI), an effluent from an abandoned mine portal in Tharsis mine (CA) and an outflow from an acidic pit lake in a big open pit in San Telmo mine (ST). The pH and Cu concentration of these samples are provided in Table 1. A common feature of these three mine waters was their high acidity (pH 2.5–2.9). They differed, however, as regards to their oxidation state (Eh = 570–750 mV), as well in sulfate and metal concentration, including dissolved copper (23–183 mg/L Cu).

Table 1. Selected chemical parameters of the three samples of acidic mine water used in this study.

Sample	pH	Eh	SO_4	Fe	Cu
		mV	mg/L	mg/L	mg/L
TI	2.6	570	23,300	1290	183
CA	2.5	615	3700	1250	124
ST	2.9	750	3350	125	23

These waters were all filtered on site through 0.45 µm pore size, nitrocellulose membrane filters (Millipore) and stored at 4 °C during transport to the laboratory. Once in the IGME Geochemistry lab, the waters were used for different experiments aimed at reducing the dissolved Cu^{2+} ions present in the acidic liquors to obtain metallic, zero-valence copper (Cu[0]). We used two different reduction methods, namely: (1) reduction with ascorbic acid ($C_6H_8O_6$) as the reducing agent, and (2) classic cementation method using scrap metallic iron (Fe[0]) as the reducing agent. To assess the effect of pH and temperature on crystallization kinetics, as well as on the crystallinity and particle size of metallic copper, the first method (ascorbic acid) was conducted at varying pH (1.50–3.95), temperature (25 °C to 80 °C), and ascorbic acid concentration (10 mM to 0.1 M $C_6H_8O_6$). The second method was solely conducted at pH 1.50 and 25 °C. Both reduction methods are briefly described below.

2.2. Batch Experiments of Cu^{2+} Reduction

2.2.1. Reduction with Ascorbic Acid

The selected acidic mine waters (500 mL in volume) were poured in glass flasks and placed in a magnetic stirring stage set at 400 rpm, where they were partially neutralized by dropwise addition of 1 M NaOH to increase the pH of the waters to values around 3.90–3.95 (Figure S1 in Supplemental Material). The goal of this partial neutralization was to remove all dissolved ferric iron in solution (Table 1) so that the experiments could be conducted without the presence of any colloids of Fe(III) minerals, such as schwertmannite, which are often formed in these solutions upon pH increase [22–25]. This pH limit, in addition, ensured the absence of aluminum precipitates that form in AMD systems at pH > 4.0 [26,27]. The titrated solutions were filtered in a vacuum filtration unit (Millipore) using 0.45 µm pore size filters to remove all Fe(III) precipitates (Figure S1).

The partly neutralized (pH ~3.95), acidic mine waters were subsequently titrated by dropwise addition of an ascorbic acid solution (1 M, pH 2.5). This ascorbic acid solution had been previously prepared by dilution of pure (reagent-grade), dry crystalline ascorbic acid ($C_6H_8O_6$) from Merck in ultrapure distilled water (Millipore). The addition of ascorbic acid (AA) to the MilliQ water resulted in an immediate acidification, and the increase of the AA concentration in the solution tended to attain an apparent equilibrium pH around 2.5 for AA concentrations greater than 1 g/L (Figure S2 in Supplemental Materials). This acidification was provoked by rapid deprotonation of AA and partial conversion to ascorbate through Reaction (1) [28]:

$$C_6H_8O_6 \rightarrow C_6H_7O_6^- + H^+ \quad (1)$$

Both AA and ascorbate can effectively reduce Cu(II) and Fe(III) ions, though AA reactions with transition metals such as Fe(III) or Cu(II) have rate constants that differ by up to several orders of magnitude, with the reactions of ascorbate usually being faster [28]. In any case, in this study we refer to 'ascorbic acid' to consider the total amount of the protonated form, AA, and the deprotonated form (ascorbate) present in the reducing solutions.

The pH of the solutions was continuously measured during the reduction experiments with previously calibrated CRISON pH meters, and visual changes of color and turbidity were recorded and annotated. When a metallic copper precipitate was apparently formed (based on color change or turbidity formation), the solutions were immediately filtered through 0.45 µm pore size filters and the obtained solids were washed several times by MilliQ water, and air-dried at ambient temperature for further morphological, mineralogical, and crystallographic analysis (Figure 1).

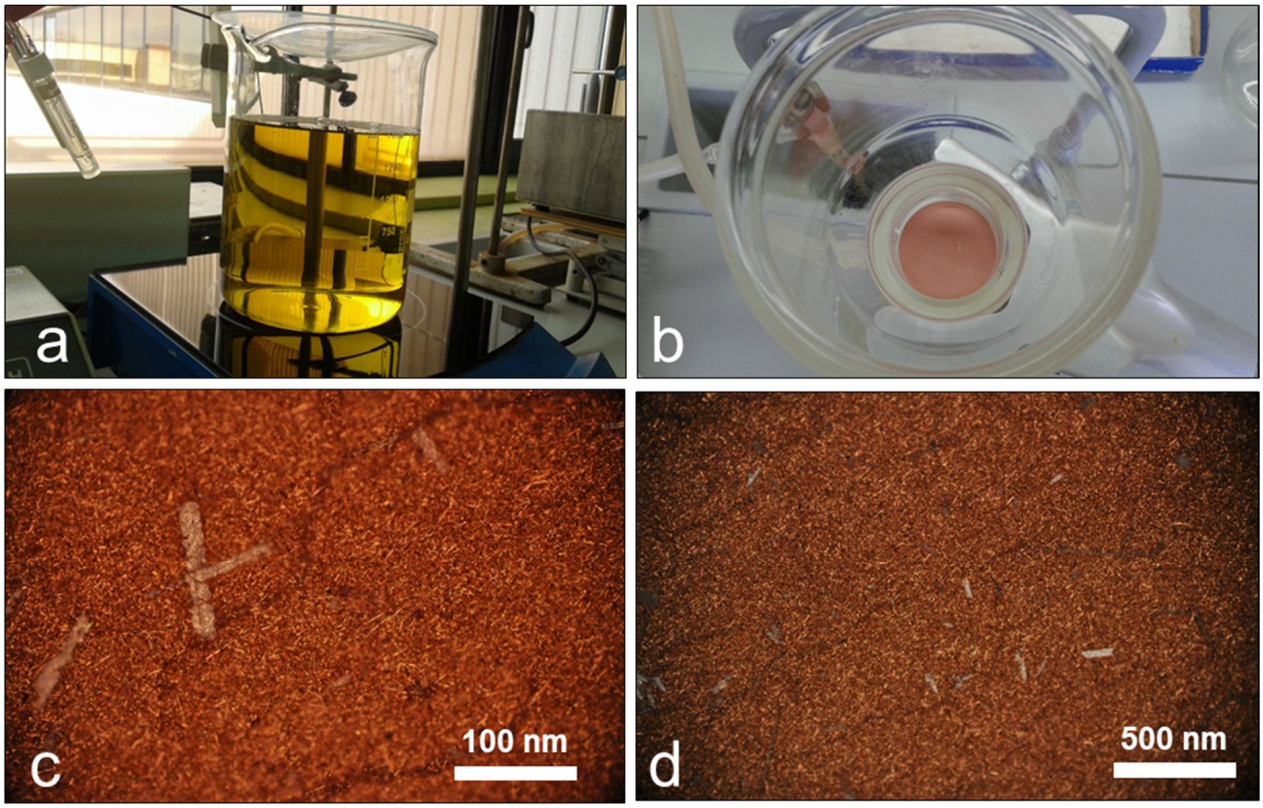

Figure 1. (**a**) Natural Cu-rich aqueous solution from AMD-affected acidic stream mixed with 10 mM AA (pH = 3.95, T = 25 °C) and containing an undetermined transient Cu complex; (**b**) Metallic copper precipitate formed on the filter after filtration of the solution shown in (**a**) after 24 h; (**c**,**d**) Reflected light microscope photomicrographs (at 500× magnification) taken on the filter shown in (**b**), showing a network of small acicular microcrystals of metallic copper (Cu[0]) along with sparse large translucent crystals of gypsum which could not be avoided (due to high Ca and SO_4 concentration in the AMD waters).

The above explained experiments at pH 3.95 and 25 °C were repeated at conditions of lower pH (1.5–2.5) and higher temperature (40–80 °C), as well as at different AA concentration (10 mM to 0.1 M) to investigate the effect of these parameters on the kinetics of Cu[0] crystallization (see Figure S3 in Supplemental Material). All experiments were conducted under oxygenic conditions.

2.2.2. Reduction with Scrap Iron

A second set of experiments was performed to obtain Cu[0] by the classical cementation method using iron as reducing agent. Instead of scrap iron we used clean nuts and screws (previously sonicated and rinsed with ethanol and MilliQ water to remove any dust or contamination from the hardware surfaces) which were submersed in the Cu^{2+}-containing acidic liquors (Supplemental Figure S4). These experiments were conducted at conditions of pH = 1.5 (after previous adjustment of the acidic solutions with H_2SO_4 1 M) and T = 25 °C, with intermittent shaking and in the presence of oxygen, until the pH and Eh values (which were continuously measured) were fully stabilized (the time elapsed in these trials was between 80 and 90 min). The pH for these experiments was adjusted to pH 1.5 following previous research which report a high efficiency of Cu[0] cementation at these very acidic conditions [4,20] and also to avoid the presence of solid-phase Fe(III) (e.g., minerals such as jarosite) which may also form in these waters at pH > 2.0 [16,17]. When the solutions had been stabilized, the iron pieces appeared fully coated by a reddish-brown colored film, and abundant blackish particles had been formed in the aqueous solution (Figure S4). These black, elongated particles were separated from the aqueous solution by vacuum filtration as discussed above. The filters were also air-dried at ambient T and were studied by XRD and SEM-EDX, as described below.

2.3. X-ray Diffraction, Optical Microscopy and Electron Microscopy

The metallic copper precipitates were analyzed by different techniques at the SGIker facilities of the University of the Basque Country (UPV/EHU). Cu[0]-coated filters were firstly examined under reflected light optical microscope Nikon Eclipse 50i/POL using a LV-UEPI Universal Epi Illuminator. X-ray diffraction (XRD) was carried out on a PANalytical X'Pert Pro diffractometer (Malvern Panalytical Ltd., Almelo, The Netherlands), with graphite monochromator, a programmable divergence slit, and a solid-state PIXcel detector. The working conditions were 40 kV and 40 mA, Cu Kα radiation and a continuous scan range of 2–90°2θ. Samples were finely grinded in an agate mortar, dispersed in ethanol and placed on zero-background Si holder. The goniometer was calibrated with a silicon standard and diffraction data processed using X'Pert High Score software with ICDD database.

The obtained precipitates were further studied by Scanning Electron Microscopy (SEM). A JEOL JSM-7000F field emission electron microscope (JEOL Ltd., Tokyo, Japan) coupled to Energy Dispersion X-ray Spectroscope (EDX) was used. Working conditions included 20 kV beam voltage, 1 nA beam current, 10 mm working distance, vacuum $< 8.35 \times 10^{-4}$ Pa. Samples were examined in both secondary electron (SE) and backscattered electron (BSE) modes with acquisition time in range of 60 to 100 s at every point of interest. Prior to SEM analysis, samples were mounted on C stab, passed through plasma cleaning process (3 min), and metalized with carbon, avoiding introducing any additional metal to the system.

2.4. Metal Concentration in the Aqueous Solutions

Metal concentrations in the aqueous solutions before and after the experiments were also conducted to quantify Cu removal during Cu(II) reduction. These analyses were performed by Inductively Coupled Plasma Atomic Emission Spectrometry (ICP-AES) in a Varian Vista-MPX spectrometer (Agilent Technologies Inc., San Clara, CA, USA).

2.5. Geochemical Modeling

The geochemical software package PHREEQCI (Version 3.0.5-7748, US Geological Survey, Reston, VA, USA [29]) was used for (1) modeling of copper ionic species in solution at varying pH and redox conditions (Eh), and (2) calculation of saturation indices (SI) of selected Cu-bearing minerals. All the calculations were conducted using the MINTEQA2 thermodynamic database (Version 4.0, USEPA, Washington, DC, USA) [30]. The saturation indices of selected copper-containing mineral phases were calculated using the correspond-

ing solubility products (log K_{sp} values) included in the MINTQA2.V4 database, as well as the known composition of the acidic waters and the experimental conditions.

3. Results

3.1. Reduction of Cu^{2+} Ions with Ascorbic Acid

The first batch reduction experiments were conducted at low AA concentration (10 mM), pH = 3.95 and T = 25 °C (Figure 1). At these conditions, the solutions turned to a yellowish color after a few minutes (Figure 1a). The color of the solution did not change after filtration through 0.45 and 0.1 μm pore size. Therefore, this color was interpreted to be diagnostic of the formation of either a transient colloidal (nano-sized) compound or an ionic complex containing Cu^{2+} or Cu^{+} ions chelated with ascorbate anion. No crystallization was observed for hours, and these solutions were left to evolve overnight at ambient temperature (25 °C). After 24 h, the solution had turned colorless, and a pinkish precipitate had been accumulated in the flask bottom. This solid, which was removed by vacuum filtration (Figure 1b) and subsequently studied by optical microscopy and XRD, consisted almost exclusively in metallic copper (Cu[0]) that was present in the form of elongated, reddish, micrometric crystals of up to 50 μm, sometimes visible to the naked eye as small reflections (Figure 1c), mingled up with much smaller equidimensional crystals (average around 2 × 2 μm).

The XRD analyses revealed the major peaks diagnostic of metallic copper (e.g., facets such as 111, 200, 220, or 311), although traces of cuprite (Cu_2O) could be also deduced by the presence of tiny peaks at around 38°2θ, corresponding to the most intense 111 facets of this mineral (Figure 2). XRD analyses of the precipitates formed in other batch experiments at higher AA concentrations revealed that metallic copper was always the final and stable mineral product resulting from the interaction of the Cu^{2+} ions with the added AA, though some tiny peaks suggestive of some minor presence of cuprite could be observed in some samples (Figure 2). Due to the use of AA in the experiments, which is a well-known antioxidant compound preventing Cu[0] oxidation [2–5], we believe that these trace amounts of Cu_2O represent remnants of a transitional cuprite nanocolloidal precursor, rather than the result of post-experimental Cu[0] oxidation.

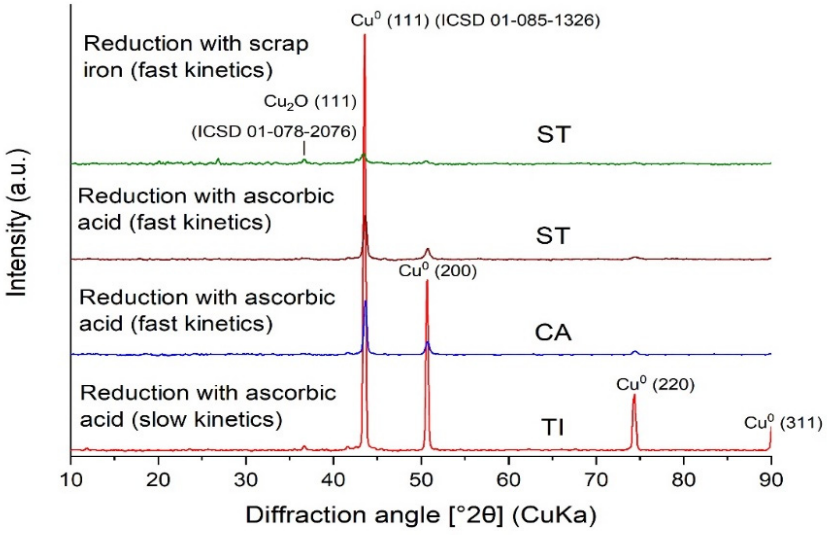

Figure 2. XRD patterns of Cu[0] obtained in the different batch experiments conducted in this study: (I) large Cu[0] crystals formed by reduction of Cu(II)-rich solutions with ascorbic acid 10 mM at pH 3.95 and 25 °C (TI; bottom), (II) Cu[0] nanoparticles formed by reduction with ascorbic acid 0.1 M at pH 3.95 and 80 °C (CA, ST; center), and (III) Cu[0] nanoparticles formed by reduction with Fe[0] (scrap iron) at pH 1.5 and 25 °C (ST; top).

The experiments conducted at pH 3.95 and AA concentrations of 0.1 M showed much faster precipitation kinetics. A dense brownish-red-colored suspension containing Cu[0] particles was formed around 5–10 min after the addition of AA (Figure S3). The reduction experiments carried out at higher T (40–80 °C) did not show a significant change in the precipitation kinetics as compared to the ones conducted at room temperature, though the reddish-brown suspensions were denser in the former case at comparable pH values. On the other hand, reduction experiments performed at low pH (1.5–2.5) did not produce either metallic copper or any other mineral product after 1 h reaction time. This is consistent with the increased electrode potential of AA at very low pH [2], which could have significantly decreased the reactions kinetics.

The lower intensity of major Cu[0] peaks (e.g., 111, 200, 220) in the XRD patterns obtained in the reduction experiments at higher AA concentration, along with faster precipitation kinetics suggested lower crystallinity degree and/or size of the Cu[0] particles (Figure 2). This hypothesis was further confirmed by the SEM-EDX studies reported in the next section.

3.2. Textural and Crystallographic Properties Revealed by Electron Microscopy

Under SEM, the Cu[0] crystals formed in the slow crystallization experiments at low AA concentration appeared with diverse morphology ranging from acicular-elongated, pseudoprismatic to isomorphic (e.g., cubes, truncated cubes, cuboctahedra), tetrahedral or truncated tetrahedra, and trapezoidal polyhedra (Figures 3 and 4). The latter ranged in size between 2–7 μm (width) and 1–4 μm (length), with a very good correlation between both dimensions (Figure 4d,e). On the other hand, pseudoprismatic and acicular-elongated crystals showed widths of around 1–4 μm but ranged largely in length between 2 and 50 μm (Figure 4b), sometimes appearing as very thin bent needle-like crystals (Figure 3a–e). Some bigger crystals showed much smaller crystallites (with varying shapes and diameters smaller than 200 nm) showing oriented growth in some of their edges or faces (e.g., Figure 3f), suggesting heterogeneous, surface-controlled crystal growth. The EDX analyses of these crystals yielded compositions of almost pure, electrolytic copper (>99% Cu; *not shown*).

In contrast to the slow kinetics–low AA concentration experiments, the fast kinetics–high AA concentration experiments produced a precipitate formed by nanometric, subrounded particles of metallic copper ranging in size between 40 and 200 nm (Figure 5). These SEM observations were in agreement with the lower crystallinity degree suggested by the XRD spectra of these samples, as described above (Figure 2). The discrete nanoparticles coalesced together in larger aggregates (with diameter of up to few microns) that could contain tens to hundreds of smaller particles (Figure 5).

3.3. Reduction of Cu^{2+} Ions with Scrap Iron

The reduction experiments using scrap iron at 25 °C and pH 1.5 resulted in the simultaneous formation of black particles in the acidic solution and a brownish-red-colored coating on the metallic pieces as the reaction proceeded (Figure S4). A high density of gas bubbles was also observed in these experiments, consistent with the production of a gaseous phase (likely hydrogen [H_2], as discussed below). Filtration of the solution after 30 min of reaction time produced a dense, black-colored precipitate (Figure S4). SEM examination of these solids revealed that these were formed by almost pure (>99%) metallic copper. In this case, metallic copper was generally present as pine-tree-like forms composed of arrays of submicron crystallites growing in diverse directions (Figure 6a–e). Less abundant forms of metallic copper produced by the cementation method included pseudo-spherical aggregates composed by coalesced, nanometric particles (<100 nm, Figure 6f) and diverse encrusting aggregates showing porous growths as boxwork-type or thin curved films (Figure 6e).

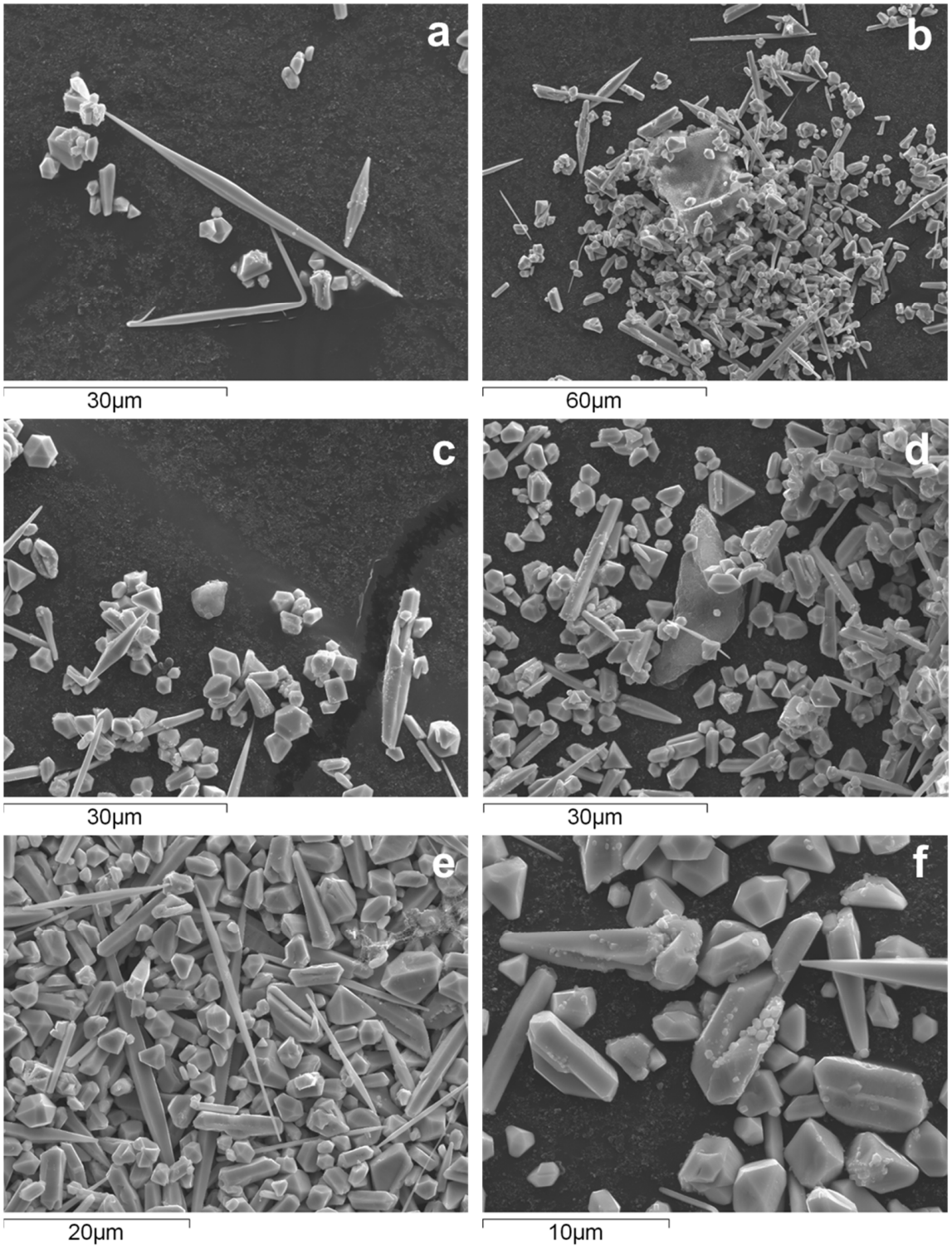

Figure 3. Scanning electron microscopy (SEM) images of the Cu crystals obtained in batch reduction experiments with Cu(II)-rich acidic solutions (pH 3.95, 25 °C) and ascorbic acid 10 mM. Pictures (**a**–**f**) display different textural and crystallographic features in a single sample (same sample as in Figure 1b,c).

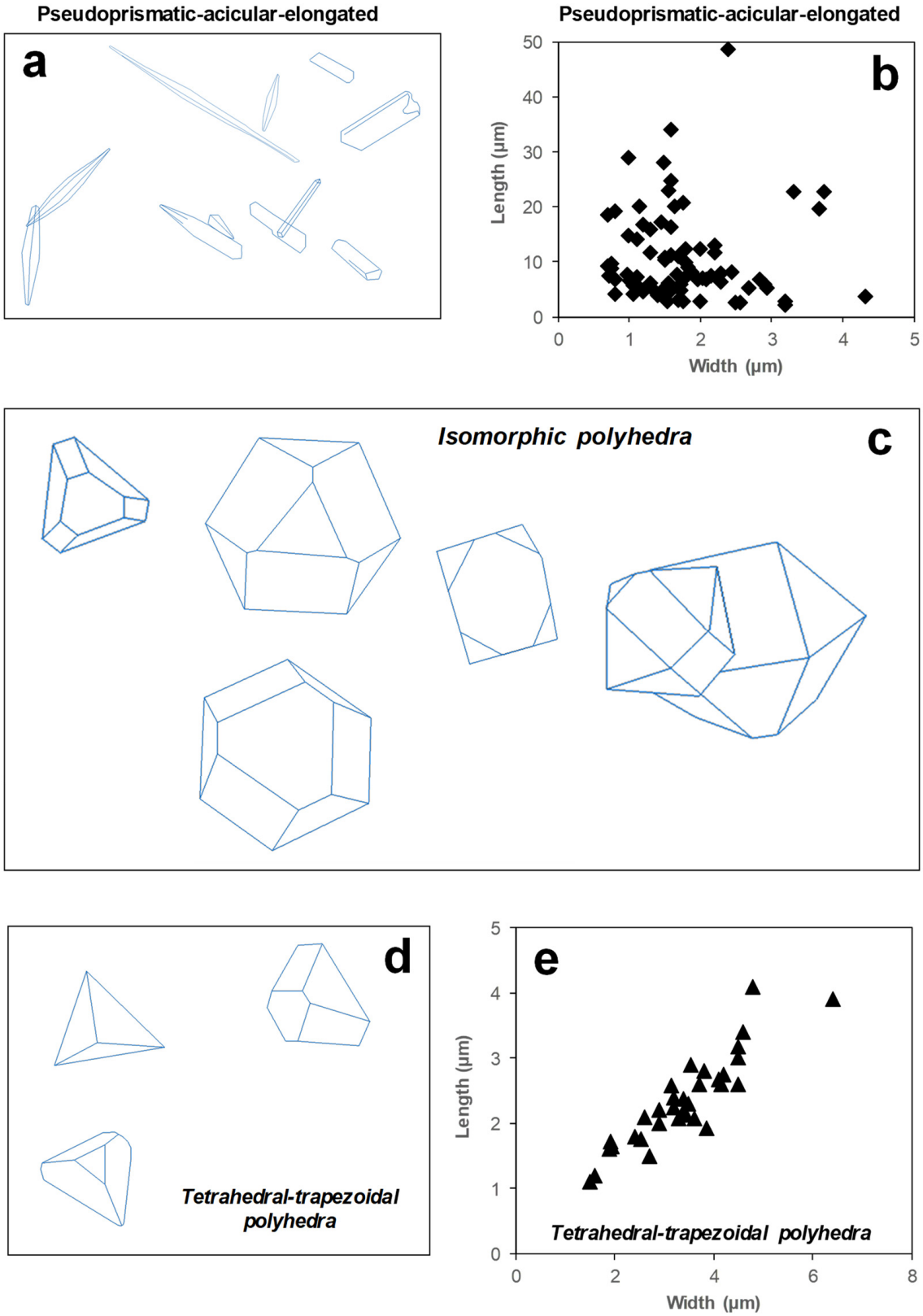

Figure 4. Geometric characteristics of different types of Cu[0] crystals formed in ascorbic acid reduction experiments (10 mM AA, pH 3.95, 25 °C) as deduced from the SEM pictures shown in Figure 3: (**a**,**b**) Pseudoprismatic-elongated-acicular crystals, (**c**) Isomorphic polyhedra, (**d**,**e**) Tetrahedral-trapezoidal polyhedra.

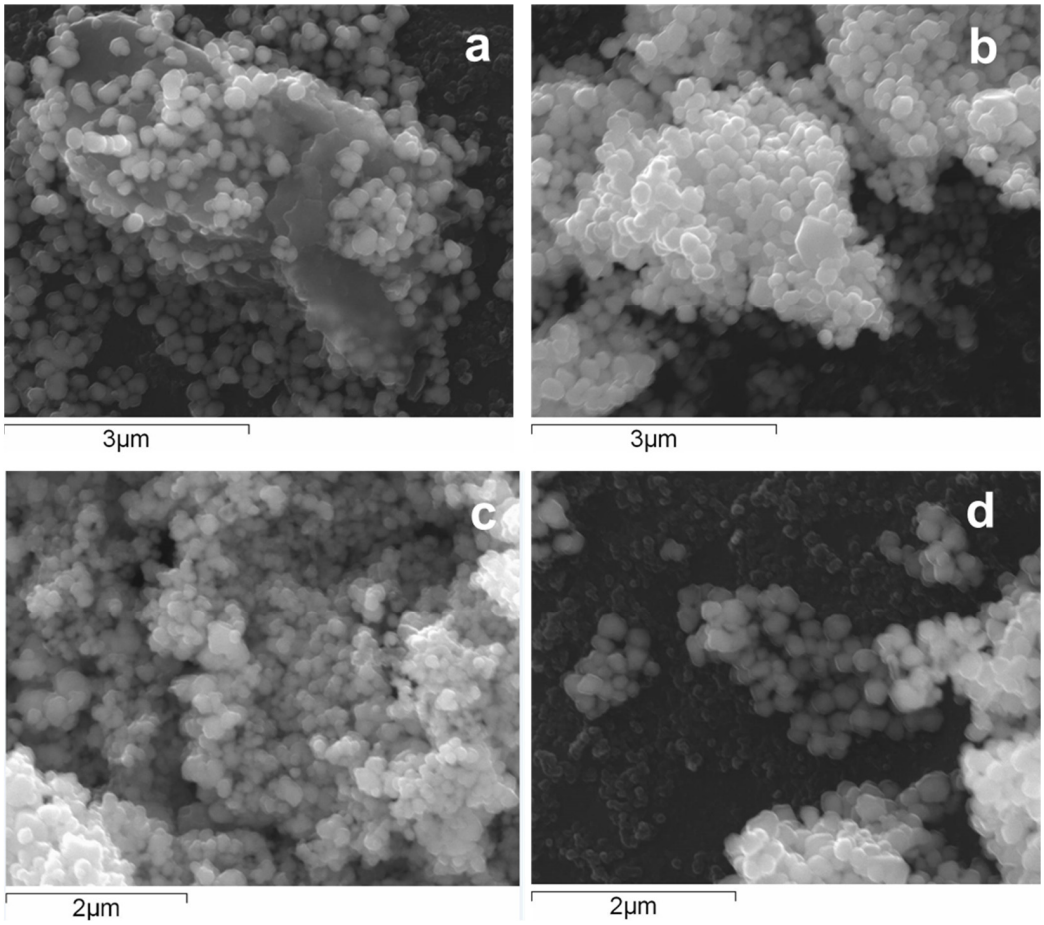

Figure 5. Scanning electron microscopy (SEM) images of metallic copper nanoparticles obtained from the reduction of Cu(II)-rich acidic solutions by ascorbic acid 0.1 M at pH 3.95 and 80 °C. (**a**,**b**) Sample CA; (**c**,**d**) Sample ST.

3.4. Metal Concentrations in the Treated Solutions

The concentration of copper (and some other major metals) was measured in the acidic solutions after the different reduction trials to compare the efficiency of the reduction treatments (Table 2). Reduction with AA was only able to recover between 15–17% (experiments with 10 mM AA) and 20–25% (experiments with 0.1 M AA) of the total dissolved Cu initially contained in the acidic solutions. On the other hand, the cementation method with scrap iron was highly efficient, with a recovery around 98% of the initial total dissolved Cu (results for TI sample are provided in Table 2 as an example). The most soluble metals (e.g., Co, Ni, Mn, Cd) behaved conservatively and remained virtually unaffected, as expected [31]. Iron was almost totally removed from solution at pH 3.95, in accordance with its known solubility behavior [22,23]. Aluminum was not totally conservative at pH 3.95 (removal of 8% of the initial Al content as a result of very limited precipitation). Finally, dissolved iron increased notably (around 12% increase) in the cementation experiment as a result of the oxidative dissolution of metallic iron (Fe[0]) to ferrous iron (Fe^{2+}).

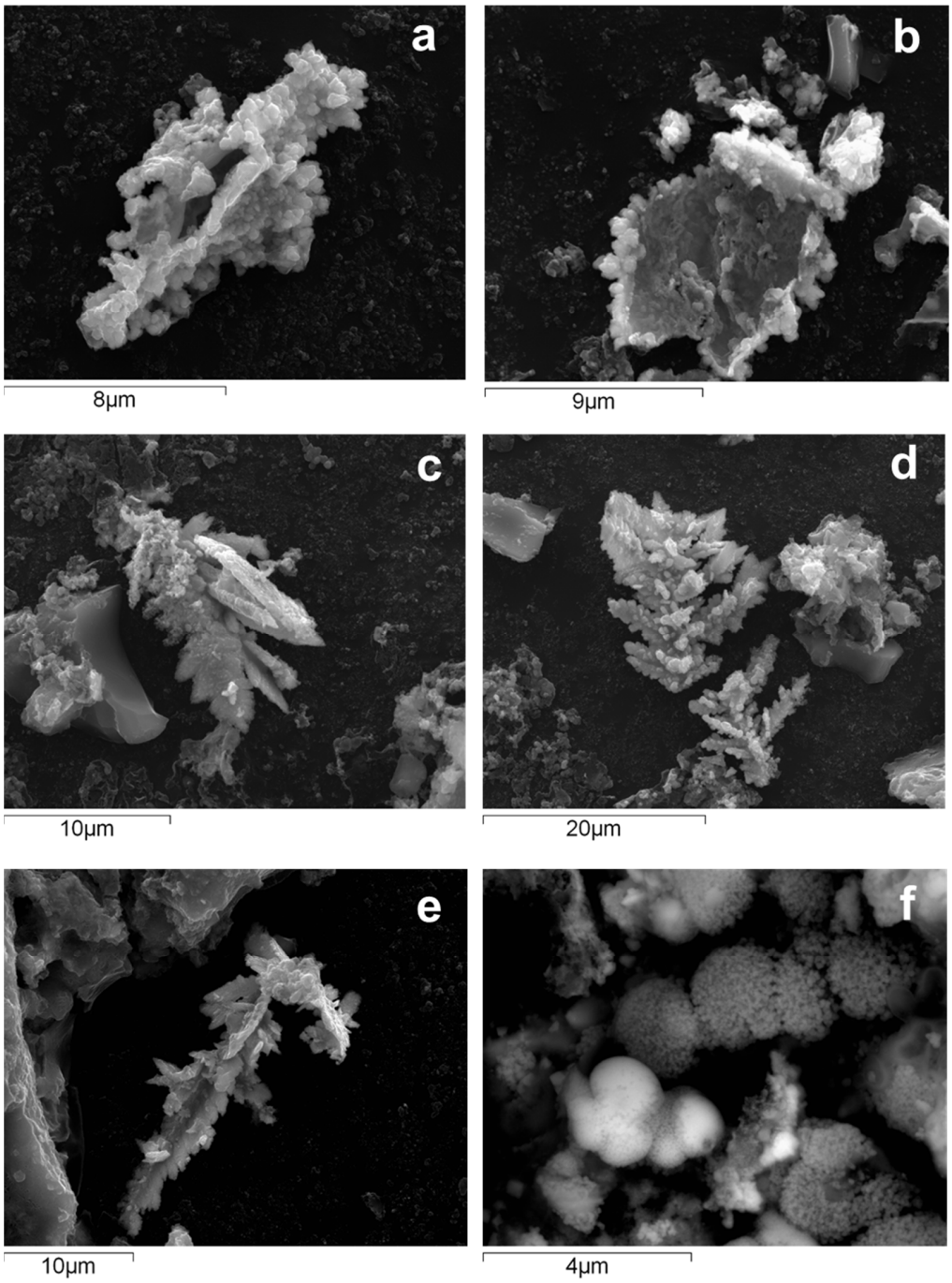

Figure 6. Scanning electron microscopy (SEM) images of metallic copper obtained in batch reduction experiments with Cu(II)-rich acidic solutions and Fe[0] (scrap iron) as reducing agent at pH 1.5. (**a**–**c**) sample TI; (**d**–**f**) sample CA; (**f**) is a BSE image of Cu[0] spheroids.

Table 2. Concentration of selected dissolved metals (in mg/L) in acidic mine water samples from TI after several Cu^{2+} reduction treatments.

	Al	Ca	Co	Cu	Cd	Fe	Ni	Mn	Zn
(1) pH 2.5	2108	455	10.10	183	2.18	1290	6.11	383	632
(2) pH 3.95 + AA 10 mM	1947	448	9.72	155	1.98	9.2	5.59	384	601
(3) pH 3.95 + AA 0.1 M	1930	447	9.80	131	1.95	8.9	5.52	382	599
(4) pH 1.50 + scrap iron	2109	453	10.05	2.62	2.01	1451	6.02	381	611

(1) original composition (previous to reduction); (2) neutralization to pH 3.95 followed by addition of AA 10 mM; (3) neutralization to pH 3.95 followed by addition of AA 0.1 M; (4) cementation with scrap iron at pH 1.50.

3.5. Geochemical Modeling

Water/mineral equilibrium calculations and theoretical distribution of Cu ionic species in solution, as deduced from PHREEQC computations, are given in Figure 7, and will be briefly discussed in this section.

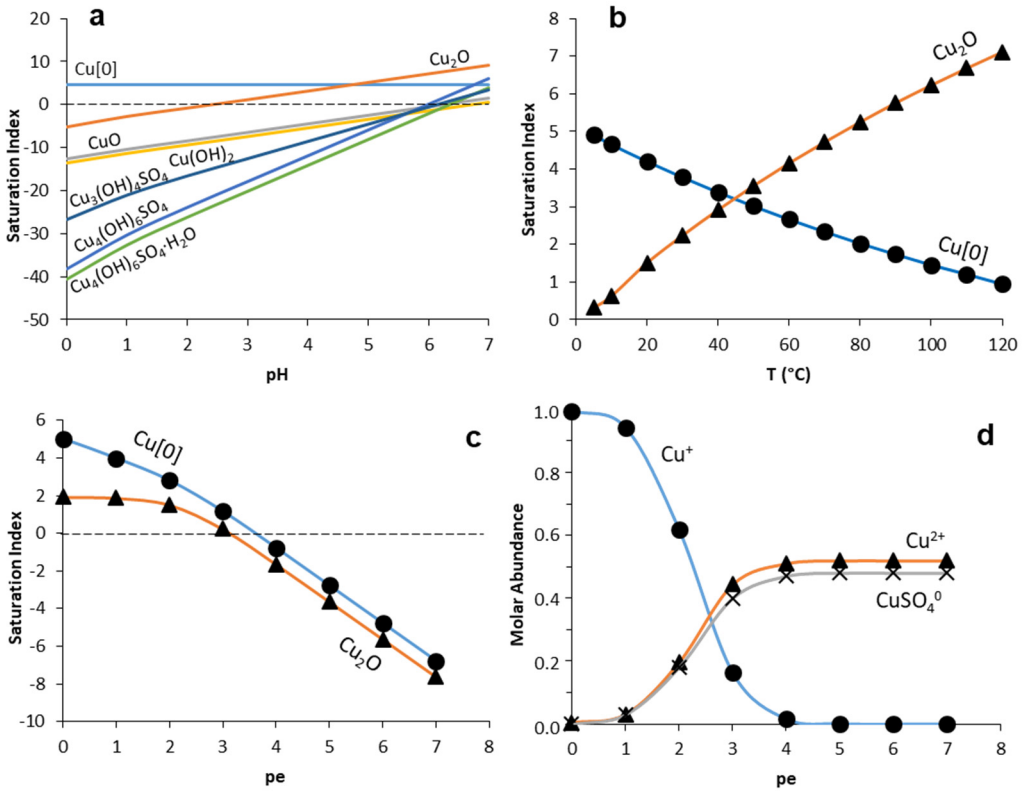

Figure 7. Water/mineral equilibrium trends in the system Cu-O-S at 1 bar: (**a**) Saturation Index of different Cu-containing phases with respect to the Cu(II)-rich acidic solution as a function of pH (pe = 1); (**b**) Evolution of the saturation index of metallic copper (Cu[0]) and cuprite (Cu_2O) as a function of temperature (T) at conditions of pH = 4 and pe = 1; (**c**) Evolution of the saturation index of Cu[0] and Cu_2O as a function of electronic potential (pe = Eh/59.2) at conditions of T = 25 °C and pH = 4; (**d**) Molar proportion of major ionic copper species in solution (Cu^+, Cu^{2+}, $CuSO_4{}^0$) as a function of pe. The computations considered in all cases Cu = 3×10^{-3} M, S = 0.2 M and $O_2 = 2 \times 10^{-4}$ M.

3.5.1. The Effect of pH

As regards pH dependency at the experimental conditions, an important difference exists between the solubility trend of copper and that shown by the rest of minerals. Our calculations for conditions of T = 25 °C and pe = 1 show that the saturation state of metallic copper is independent of pH, whereas the rest of minerals are strongly pH-dependent (Figure 7a). Thus, the Cu-rich mine waters would be saturated with respect to metallic copper in the whole pH range investigated (0–7), showing a constant saturation index (SI) around 4.0, which suggests strong thermodynamic favorability for metallic copper crystallization (Figure 7a). Conversely, the cuprous oxide (tenorite, CuO), copper hydroxide ($Cu(OH)_2$), and diverse copper oxy-hydroxysulfates ($Cu_3(OH)_4SO_4$, $Cu_4(OH)_6SO_4$, $Cu_4(OH)_6SO_4{\cdot}H_2O$) are strongly undersaturated at low pH and become saturated only at near-neutral conditions. Cuprite (Cu_2O) represents an exception among the later minerals, since it becomes saturated at pH values higher than 3.0 and shows even higher saturation than metallic copper for pH > 4.5 (Figure 7a). The solubility behavior of cuprite may, therefore, be of interest to understand the partition between dissolved and solid-state Cu in the acidic solutions during the reduction experiments at pH values comprised between 3 and 5.

The lowest pH conditions (<2.0) clearly favor the formation of metallic copper by reduction of Cu^{2+} ions, provided that redox conditions are suitable (i.e., sufficiently low Eh or pe). It is worth noting that these calculations only consider thermodynamic favorability and tendency to precipitation and do not take into account kinetic considerations. Therefore, a positive and high SI for Cu[0] at a given pH does not necessarily imply copper nucleation and crystallization, especially if the formation of some other solid phase (e.g., Cu_2O) has faster precipitation kinetics and/or lower activation energy barriers.

3.5.2. The Effect of Temperature

Metallic copper and cuprite show inverse trends as regards to temperature dependence of their solubilities (Figure 7b). In the window of 0–120 °C (conditions of pH = 4, pe = 1 and 10 μM O_2), the saturation index of Cu[0] decreases continuously from a maximum value around 5 at 0 °C to a minimum value around 1 at 120 °C. An opposite trend is observed for cuprite, which shows a continuous SI increase from values around 0 at 0 °C to values around 7.5 at 120 °C. In this case, the reduction of Cu^{2+} at room temperature will be always more convenient than at higher T since these conditions favor the formation of elemental copper with respect to cuprite.

3.5.3. The Effect of Redox Potential

The PHREEQC calculations also revealed the strong dependence of copper speciation and precipitation on the redox conditions (Figure 7c,d). Copper is mostly present as Cu(II) (including the free cation, Cu^{2+}, and the uncharged sulfate complex, $CuSO_4^0$) for pe greater than 4.0 (Eh > 230–240 mV) (Figure 7d). Conversely, copper is almost exclusively present as the monovalent cation, Cu^+, for pe < 1 (Eh < 60 mV). It is important to note, however, that these calculations are valid for the system Cu-O-S, since they did not consider the presence of ligands other than sulfate, such as, for example, chloride, which can be bonded to both Cu^+ and Cu^{2+} to form different complexes not considered in this study. The precipitation of both metallic copper and cuprite also require reducing conditions to occur (pe < 3.5–4 for Cu[0] and pe < 3 for Cu_2O at pH = 4; Figure 7c).

Overall, the presented geochemical calculations suggest that the ideal conditions to obtain pure metallic copper crystals from the studied mine waters by reduction of Cu^{2+} should include very low pH (<2.0), low redox (pe < 1) and room temperature. These observations are in line with stability Eh/pH diagrams reported in previous studies by different authors [32] (see Figure S5 in the Supplemental Material) and point to the cementation method with reduction by scrap iron as the one with ideal conditions for Cu[0] recovery.

4. Discussion

4.1. Performance of Cu(II) Reduction by Ascorbic Acid

At near-neutral pH, AA is usually oxidized by reactive oxygen species (ROS) such as hydroxyl radicals, losing one electron to form a radical cation and then a second electron to form dehydroascorbic acid (Reaction (2)) [28,33,34]:

$$RO^{\bullet} + C_6H_7O_6^- \rightarrow RO^- + C_6H_7O_6^{\bullet} \rightarrow ROH + C_6H_6O_6 \quad (2)$$

At low pH and in the presence of transition metals such as Cu(II), however, ascorbic acid and ascorbate can be both oxidized by metal ions (e.g., Cu^{2+}) through Reactions (3) and (4), which results in the formation of dehydroascorbic acid, metallic copper, and protons [28]:

$$C_6H_8O_6 + Cu^{2+} \rightarrow C_6H_7O_6^- + Cu[0] + H^+ \quad (3)$$

$$C_6H_7O_6^- + Cu^{2+} \rightarrow C_6H_6O_6 + Cu[0] + H^+ \quad (4)$$

The overall reaction can be written as:

$$C_6H_8O_6 + Cu^{2+} \rightarrow C_6H_6O_6 + Cu[0] + 2H^+ \quad (5)$$

The stoichiometry of Reaction (5) reflects the release of two protons (H^+) per mol of ascorbic acid transformed to dehydroascorbic acid, which is in good agreement with the strong pH buffering observed in the acidic solutions at pH values between 3.65–3.70 and 3.85–3.90 during AA addition, when the solutions turned from a yellowish to a pink to reddish brown color and turbidity became evident in the flasks (Figure S3).

The absence of Cu crystallization at low pH (<3.85) and the low yield of Cu recovery at pH 3.95 is in accordance with previous studies which indicate that reduction of Cu^{2+} ions by AA is highly favored at neutral to alkaline pH [2,3]. However, some authors have previously noted that Cu^{2+} reduction by ascorbic acid can also take place at very low pH [35–37]. For example, Gonçalves et al. (2020) [35] used solutions of copper sulfate with ascorbic acid 0.1 M at pH of 1.0 to 11.0, with the solution being subjected to constant stirring at 185 rpm, without inert gas protection and at 65 °C during 22 h. These authors found a clear pH dependence of the size of Cu[0] particles: Cu[0] formed at pH 1.0 and pH 3.0 crystallized in the form of small (micrometric) platy crystals, whereas the experiments at high pH (5.0 and 7.0) resulted in granular nanoparticles [35]. Liu et al. (2012) [36] also investigated the effect of pH (3.0–11.0) in Cu nanoparticles produced by reducing Cu^{2+} ions with ascorbic acid 1 M using 15 mM polyvinylpyrrolidone as a dispersant. These authors concluded that the average size of Cu nanoparticles was strongly influenced by pH, since Cu[0] particles formed at pH 3.0 were significantly bigger than those formed at pH 5.0, which were in turn bigger than those produced at pH 7.0. Liu et al. [36] did not manage to produce Cu[0] nanoparticles at pH 9.0 and 11.0. Interestingly, the reduction of Cu^{2+} ions was found to proceed via the formation of an intermediate Cu_2O precursor, and the size of the transitional Cu_2O was also found to control the size of the Cu nanoparticles [36]. Finally, Wu (2007) [37] also managed to produce metallic copper fine powder from copper sulfate solutions at pH 2.2 and T = 50–70 °C using ascorbic acid 0.4 M, noting that the obtained polyhedral particles were significantly bigger in size than those formed at pH 6, a fact that this author attributed to the lower concentration and distinct chemical form of copper ($Cu(OH)_2$ instead of Cu^{2+}) at the higher pH values.

In the present study, the large size and well-developed faces of the Cu[0] crystals formed in the AA reduction experiments at low concentration and slow precipitation kinetics suggest a very slight degree of saturation of the solution with respect to Cu[0] solubility, which would have resulted in a low density of nucleation centers which could have enabled extensive crystal growth [37,38]. We speculate with the possibility of scarce colloidal particles of Fe(III) (<100 nm in diameter) still remaining in the solution after filtration acting as seeds or nucleation centers favoring heterogeneous precipitation of Cu[0] at the colloid surface. This possibility, however, cannot be demonstrated with the available data and would require further research.

The geochemical trends of SI shown in Figure 7a, whereby cuprite (Cu_2O) precipitation if thermodynamically favored at pH > 3.0, and the detection by XRD of trace amounts of this mineral (Figure 2) along with higher O peak in SEM-EDX in some samples may also indicate that the formation of Cu[0] could have taken place in two steps with cuprite nanocolloids being a first, transitional solid form of Cu produced by reaction with AA, which would have been subsequently transformed to Cu[0] by further interaction with AA during the following hours (Reactions (6) and (7)):

$$C_6H_8O_6 + 2Cu^{2+} + H_2O \rightarrow C_6H_6O_6 + Cu_2O + 4H^+ \quad (6)$$

$$C_6H_8O_6 + Cu_2O \rightarrow C_6H_6O_6 + 2Cu[0] + H_2O \quad (7)$$

This hypothesis would be in accordance with previous studies reporting a high efficiency of AA to convert Cu_2O nanocolloid to Cu[0] nanocolloid at different pH from acidic to neutral [3,39]. Jacukowicz-Sobala et al. [39] have also recently reported a size-controlled transformation of Cu_2O into Cu[0] within a matrix of anion exchangers via green chemical reduction whereby the preformed Cu_2O particles served as templates for the final Cu[0] particles. The much lower pH in our Cu^{2+} reduction experiments, along with the presence

of oxygen and the absence of any stabilizing agent commonly used in Cu^{2+} reduction studies (e.g., polyvinylpyrrolidone [9]) could have established ideal conditions for the formation of the unusually well-developed Cu[0] crystals obtained in the slow kinetics assays. There is a close similarity of crystal geometry between the Cu[0] crystals obtained in the present study and the Cu_2O polyhedrons found in other studies [9]. Both Cu_2O and Cu[0] crystallize in the hexoctahedral class within the isometric system [40], so that the transformation would be isomorphic through the loss of oxygen atoms from the cuprite crystal lattice.

The assays at higher AA concentrations yielded faster precipitation kinetics (formation of turbidity provoked by tiny Cu[0] particles after reaction times of minutes instead of hours) and better rates of Cu recovery from the solutions (up to 25% instead of 15% recovery of the total Cu^{2+} ions originally present in the solutions). This faster precipitation kinetics resulted in the formation of submicron to nano-sized, subrounded particles with diameters between 100 and 200 nm. In this case, the very high AA to Cu^{2+} ratio in these experiments ($C_6H_8O_6/Cu^{2+}$ = 20), as compared to the one of the low AA concentration assays ($C_6H_8O_6/Cu^{2+}$ = 2), would have led to faster complexation of the Cu^{2+} ions with either AA or ascorbate anions (Reactions (3) and (4)) [41] and to the formation of a high density of nucleation centers, leading to much smaller Cu[0] particles showing much lesser crystalline order. The presence of chloride in the AMD solutions (in the order of hundreds of mg/L Cl [16]; *not shown*) could have limited the recovery of Cu[0] in these experiments, since this salt has been shown to inhibit oxidation of ascorbic acid by transition metals such as Fe or Cu [33]. In any case, these low yields of Cu recovery coupled to the relatively high cost of chemical reagents ($C_6H_8O_6$, NaOH) needed to achieve the chemical reduction of dissolved copper in the studied solutions, probably makes this method economically impractical in very acidic mine waters such as the ones used in the present study.

4.2. Performance of Cu(II) Reduction by Scrap Iron

The classic cementation method has been historically used in the Riotinto area and many other mines in SW Spain since the XVIII century [20]. This reduction mechanism takes advantage of the very different standard reduction potentials of copper and iron [42]:

$$Cu^{2+} + 2e^{-} \rightarrow Cu[0]\ (E^0 = +340\ mV) \quad (8)$$

$$Fe^{2+} + 2e- \rightarrow Fe[0]\ (E^0 = -440\ mV) \quad (9)$$

While in contact with scrap iron (e.g., in cementation channels build for that purpose), copper ions (Cu^{2+}) become reduced on metal iron surfaces, while the corresponding amount of iron dissolves as Fe^{2+} through Reaction (10):

$$Cu^{2+} + Fe[0] \rightarrow Cu[0] + Fe^{2+} \quad (10)$$

In the presence of sulfuric acid (H_2SO_4)-rich solutions, such as the ones used in the present study, scrap iron etches and produces iron sulfate ($FeSO_4$) and molecular hydrogen (H_2) through Reaction (11) [42]:

$$Fe[0] + H2SO4 \rightarrow FeSO4 + H_2 \quad (11)$$

The intense green color (usually diagnostic of the presence of dissolved ferrous iron) attained by the acidic solutions after the reaction with scrap iron, and the intense bubbling observed during the reactions (Figure S4a), indicate that Reactions (10) and (11) occurred simultaneously during our experiments. The structure of the Cu[0] aggregates, formed by hundreds of micro-crystallites oriented in arrays growing in different directions (Figure 6) is in good agreement with a surface-controlled mechanism whereby the Cu[0] clusters formed by reduction of Cu^{2+} ions on the iron surfaces nucleate at those surfaces and crystal growth occurs.

The high yield of Cu recovery in these assays (>98%) in short reaction times of around 90 min, along with the very low cost of the reducing agent, makes this mechanism much more efficient and cheaper than the ones based in chemical reduction using AA or any other reducing agent, such as glucose or hydrazine hydrate. The high purity of metallic copper aggregates (>99% Cu[0]) obtained by this technique and the very little requirements (e.g., good performance even at very low pH, no need for expensive chemical reagents, no need for high temperature or intense stirring, etc.) makes cementation the easiest and simplest method of Cu recovery from Cu-rich mine waters and their acidic leachates.

5. Conclusions

The current practices in different industrial sectors focused on Cu recovery from different wastes include Cu^{2+} reduction by ascorbic acid as a feasible and apparently efficient technology. At the same time, there is an important need to develop cost-effective strategies of metal recovery in abandoned mine sites within the framework of circular economy and mine waste recycling [10,15]. An obvious question, therefore, emerges about the convenience of ascorbic acid-based procedures to recover Cu from acidic mine waters containing high concentrations of this metal as dissolved loadings.

We provide here, for the first time, a comparison of metallic copper products obtained by two different reduction methods from Cu-rich acid mine waters. The present work has shown that high-purity metallic copper can also be obtained from highly acidic, metal-rich mine drainage solutions by reduction of dissolved Cu^{2+} by ascorbic acid. This procedure may result in the formation of either (i) well-developed large crystals or (ii) much smaller rounded particles of sub-micron to nanometric diameter, depending on the crystallization kinetics and saturation state, which have been observed to vary with the ascorbic acid concentration used, as well as with other parameters such as pH or temperature. Compared to previous studies [2–9,34–36], we have identified a surprisingly high diversity of crystal geometries (e.g., from acicular to polyhedral) and sizes (from <200 nm to >50 μm) when using low concentrations of AA and slow crystallization kinetics. However, this procedure shows a low efficiency as regards to metal recovery rates (<25%) at the pH conditions (1.50–3.95) and AA concentrations (10 mM–0.1 M) considered in this study. This method presents some other disadvantages, such as the need of a previous partial neutralization to increase the Cu-reduction kinetics, or the undesirable removal of Cu^{2+} by adsorption on Al colloids formed in these waters at pH > 4.0. These two limitations leave a narrow operational pH window for on-site treatments in abandoned mine sites. In any case, the possibility of controlling crystal geometry or particle size as a function of varying experimental conditions (e.g., pH, T, [Cu/AA] ratio) could make this procedure still interesting if further improvements are conducted to increase its efficiency.

In contrast, the classical cementation method of Cu^{2+} reduction by scrap iron, historically applied in the IPB and other mine districts [20,21], offers an easier, cheaper, and more effective option of Cu recovery from mine waters. The metallic copper produced by this method is also highly crystalline, although commonly forms aggregates of smaller crystallites than those formed by the slow kinetics ascorbic acid method. The big advantages of the cementation method are: (i) it can be applied at very low pH (thus, with no need of alkalization), and (ii) it does not require expensive reagents. Therefore, this method could be used in combination with some other techniques in a multi-metal recovery scheme aimed at obtaining secondary raw materials or at least at defraying remediation treatment costs.

Supplementary Materials: The following supporting information can be downloaded at: https://www.mdpi.com/article/10.3390/min12030322/s1, Figure S1: Pictures on partial neutralization of AMD water prior to Cu^{2+} reduction experiments; Figure S2: Plot of pH vs ascorbic acid concentration; Figure S3: Cu^{2+} reduction experiments at higher pH and ascorbic acid concentration; Figure S4: Pictures showing one of the experiments of Cu^{2+} reduction using iron (Fe[0]) metallic pieces; Figure S5: Eh/pH diagrams for the Cu-O-H system using different thermodynamic databases.

Author Contributions: Conceptualization, J.S.-E.; Methodology, J.S.-E.; Validation, J.S.-E., I.Y. and A.I.; Formal Analysis, J.S.-E., I.Y. and A.I.; Investigation, J.S.-E., I.Y. and A.I.; Resources, J.S.-E. and I.Y.; Data Curation, J.S.-E. and A.I.; Writing—Original Draft Preparation, J.S.-E.; Writing—Review and Editing, J.S.-E., I.Y. and A.I.; Project Administration, J.S.-E.; Funding Acquisition, J.S.-E. All authors have read and agreed to the published version of the manuscript.

Funding: This research was funded by the Spanish Ministry of Science and Innovation through grant number CGL2016-74984-R.

Acknowledgments: We acknowledge the technicians and staff at the Geochemistry Laboratory at IGME-CSIC for their kind help and support during the experimental work. We also thank the personnel at the SGIker facilities at UPV/EHU for their support during the XRD and SEM analyses. We are grateful to two anonymous reviewers who helped improve this manuscript.

Conflicts of Interest: The authors declare no conflict of interest. The funders had no role in the design of the study; in the collection, analyses, or interpretation of data; in the writing of the manuscript, and in the decision to publish the results.

References

1. Ghosh, S. Electroless copper deposition: A critical review. *Thin Solid Films* **2019**, *669*, 641–658. [CrossRef]
2. Saikova, S.V.; Murasheva, K.S.; Vorobyev, S.A.; Kochmarev, K.Y.; Karimov, E.E.; Eremina, A.D.; Mikhlin, Y.L. Synthesizing highly concentrated hydrosols of copper nanoparticles via reduction by ascorbic acid in the presence of gelatose. *Chem. Sust. Dev.* **2013**, *21*, 403–409.
3. Andal, V.; Buvaneswari, G. Effect of reducing agents in the conversion of Cu_2O nanocolloid to Cu nanocolloid. *Eng. Sci. Technol.* **2017**, *20*, 340–344. [CrossRef]
4. Kumar, S.; Kumar, V.; Sharma, M.L.; Chakarvarti, S.K. Electrochemical synthesis of metallic micro-rose having petals in nanometer dimensions. *Superlattice Microstruct.* **2008**, *43*, 324–329. [CrossRef]
5. Tsai, C.-Y.; Chang, W.-C.; Chen, G.-L.; Chung, C.-H.; Liang, J.-X.; Ma, W.-Y. A study of the preparation and properties of antioxidative copper inks with high electrical conductivity. *Nanoscale Res. Lett.* **2015**, *10*, 357. [CrossRef] [PubMed]
6. Virk, H.S. Fabrication and characterization of metallic copper and copper oxide nanoflowers. *Pak. J. Chem.* **2011**, *1*, 148–154. [CrossRef]
7. Virk, H.S.; Kishore, K.; Balouria, V. Fabrication of copper nanowires by electrodeposition using anodic alumina and polymer templates. *J. Nano Res.* **2010**, *10*, 63–67. [CrossRef]
8. Sarkar, J.; Khan, G.G.; Basumallick, A. Nanowires: Properties, applications and synthesis via porous anodic aluminum oxide template. *Bull. Mater. Sci.* **2007**, *30*, 271–290. [CrossRef]
9. Zhang, D.-F.; Zhang, H.; Guo, L.; Zheng, K.; Han, X.-D.; Zhang, Z. Delicate control of crystallographic facet-oriented Cu_2O nanocrystals and the correlated adsorption ability. *J. Mater. Chem.* **2009**, *19*, 5220–5225. [CrossRef]
10. Lottermoser, B.G. Recycling, Reuse and Rehabilitation of Mine Wastes. *Elements* **2011**, *7*, 405–410. [CrossRef]
11. Nordstrom, D.K.; Alpers, C.N. Geochemistry of acid mine waters. In *The Environmental Geochemistry of Mineral Deposits, Part A*; Processes, Techniques, and Health Issues; Plumlee, G.S., Logsdon, M.J., Eds.; Society of Economic Geologists: Littleton, CO, USA, 1999; Volume 6, pp. 133–156.
12. Geller, W.; Klapper, H.; Schultze, M. Natural and anthropogenic sulphuric acidification of lakes. In *Acidic Mining Lakes–Acid Mine Drainage, Limnology and Reclamation*; Geller, W., Klapper, H., Salomons, W., Eds.; Springer: Berlin/Heidelberg, Germany, 1998; pp. 3–14.
13. Barthen, R.; Sulonen, M.L.K.; Peräniemi, S.; Jain, R.; Lakaniemi, A.M. Removal and recovery of metal ions from acidic multi-metal mine water using waste digested activated sludge as biosorbent. *Hydrometallurgy* **2022**, *207*, 105770. [CrossRef]
14. Isosaari, P.; Sillampää, M. Use of Sulfate-Reducing and Bioelectrochemical Reactors for Metal Recovery from Mine Water. *Sep. Purif. Rev.* **2014**, *46*, 1–20. [CrossRef]
15. León, R.; Macías, F.; Cánovas, C.; Pérez-López, R.; Ayora, C.; Nieto, J.M.; Olías, M. Mine waters as a secondary source of rare earth elements worldwide: The case of the Iberian Pyrite Belt. *J. Geochem. Exp.* **2021**, *224*, 106742. [CrossRef]
16. Sánchez-España, F.J.; López Pamo, E.; Santofimia, E.; Aduvire, O.; Reyes, J.; Barettino, D. Acid Mine Drainage in the Iberian Pyrite Belt (Odiel river watershed, Huelva, SW Spain): Geochemistry, Mineralogy and Environmental Implications. *App. Geochem.* **2005**, *20*, 1320–1356. [CrossRef]
17. Sánchez España, J.; López Pamo, E.; Santofimia, E.; Diez-Ercilla, M. The acidic mine pit lakes of the Iberian Pyrite Belt: An approach to their physical limnology and hydrogeochemistry. *App. Geochem.* **2008**, *23*, 1260–1287. [CrossRef]
18. López-Pamo, E.; Sánchez-España, J.; Santofimia, E.; Diez-Ercilla, M.; Reyes, J. *Cortas Mineras Inundadas de la Faja Pirítica: Inventario e Hidroquímica*; Instituto Geológico y Minero: Madrid, Spain, 2009; 279p.
19. Sánchez-España, J.; Diez, M.; Santofimia, E. Mine pit lakes of the Iberian Pyrite Belt: Some basic limnological, hydrogeochemical and microbiological considerations. In *Acidic Pit Lakes: The Legacy of Coal and Metal Surface Mines*; Geler, W., Ed.; Springer: Berlin/Heidelberg, Germany, 2013; pp. 315–342.

20. Taylor, J.H.; Whelan, P.F. The leaching of cupreous pyrites and the precipitation of copper at Rio Tinto, Spain. *Trans. Inst. Min. Metall.* **1943**, *52*, 35–96.
21. Tucci, N.J.; Gammons, C.H. Influence of copper recovery on the water quality of the acidic Berkeley Pit lake, Montana, U.S.A. *Environ. Sci. Technol.* **2015**, *49*, 4081–4088. [CrossRef]
22. Bigham, J.M.; Nordstrom, D.K. Iron and Aluminum Hydroxysulfates from Acid Sulfate Waters. In Sulfate Minerals: Crystallography, Geochemistry, and Environmental Significance. *Rev. Mineral. Geochem.* **2000**, *40*, 351–403. [CrossRef]
23. Sánchez-España, J. The behavior of iron and aluminum in acid mine drainage: Speciation, mineralogy, and environmental significance. In *Thermodynamics, Solubility and Environmental issues*; Letcher, T., Ed.; Elsevier: Amsterdam, The Netherlands, 2007; pp. 137–150.
24. Sánchez-España, J.; López-Pamo, E.; Santofomia, E.; Reyes, J.; Martín-Rubí, J.A. The removal of dissolved metals by hydroxysulphate precipitates during oxidation and neutralization of acid mine waters, Iberian Pyrite Belt. *Aquat. Geochem.* **2006**, *12*, 269–298. [CrossRef]
25. Sánchez-España, J.; Yusta, I.; López, G. Schwertmannite to jarosite conversion in the water column of an acidic mine pit lake. *Mineral. Mag.* **2012**, *76*, 2659–2682. [CrossRef]
26. Nordstrom, D.K. The effect of sulphate on aluminum concentrations in natural waters: Some stability relations in the system Al_2O_3-SO_3-H_2O at 298 K. *Geochim. Cosmochim. Acta* **1982**, *46*, 681–692. [CrossRef]
27. Sánchez-España, J.; Yusta, I.; Burgos, W.D. Geochemistry of dissolved aluminum at low pH: Hydrobasaluminite formation and interaction with trace metals, silica and microbial cells under anoxic conditions. *Chem. Geol.* **2016**, *441*, 124–137. [CrossRef]
28. Shen, J.; Griffiths, P.T.; Campbell, S.J.; Utinger BKalberer, M.; Paulson, S.E. Ascorbate oxidation by iron, copper and reactive oxygen species: Review, model development, and derivation of key rate constants. *Sci. Rep.* **2021**, *11*, 7417. [CrossRef] [PubMed]
29. Parkurst, D.L.; Appelo, C.A.J. User's guide to PHREEQC (version 2)—A computer program for speciation, batch-reaction, one-domensional transport, and inverse geochemical calculations. In *U.S. Geological Survey Water-Resources Investigations Report 99-4259*; U.S. Geological Survey: Denver, CO, USA, 1999; 312p.
30. Allison, J.D.; Brown, D.S.; Novo-Gradac, J. *MINTEQA2/PRODEAFA2, A Geochemical Assessment Model for Environmental Systems: User Manual Supplement for Version 4.0*; U.S. Environmental Protection Agency: Athens, GA, USA, 1999.
31. Sánchez-España, J.; Yusta, I. Low-crystallinity products of trace-metal precipitation in neutralized pit-lake waters without ferric and aluminous adsorbent: Geochemical modelling and mineralogical analyses. *Mineral. Mag.* **2015**, *79*, 781–798. [CrossRef]
32. Takeno, N. Atlas of Eh-pH diagrams: Intercomparison of thermodynamic databases. In *Geological Survey of Japan Open File Report No. 419*; National Institute of Advanced Industrial Science and Technology: Tokyo, Japan, 2005; 285p.
33. Mystkowski, E.M. The oxidation of ascorbic acid in the presence of copper. *Biochem, J.* **1942**, *36*, 494–500. [CrossRef]
34. Hacisevkí, A. An overview of ascorbic acid biochemistry. *J. Fac. Pharm. Ank.* **2009**, *38*, 233–255.
35. Goçalves, T.A.; Botelho, A.B.; de Moraes, V.T.; Espinos, D.C.R. Study of pH Influence in the Synthesis of Copper Nanoparticles Using Ascorbic Acid as Reducing and Stabilizing Agent. In *Proceedings of the TMS 2020 149th Annual Meeting & Exhibition, San Diego, CA, USA, 23–27 February 2020*; The Minerals, Metals & Materials Society, Ed.; The Minerals, Metals & Materials Series; Springer Nature: Cham, Switzerland, 2020; pp. 1547–1557.
36. Liu, Q.M.; Yasunami, T.; Kuruda, K.; Okido, M. Preparation of Cu nanoparticles with ascorbic acid by aqueous solution reduction method. *Trans. Nonferrous Met. Soc. China* **2012**, *22*, 2198–2203. [CrossRef]
37. Songping, W. Preparation of fine copper powder using ascorbic acid as reducing agent and its application in MLCC. *Mater. Lett.* **2017**, *61*, 1125–1129. [CrossRef]
38. Sánchez-España, J. Crystallization in acidic media: From nanoparticles to macrocrystals. *Semin. Soc. Esp. Mineral.* **2017**, *13*, 15–34.
39. Jacukowicz-Sobala, I.; Stanisławska, E.; Baszczuk, A.; Jasiorski, M.; Kociołek-Balawejder, E. Size-Controlled Transformation of Cu_2O into Zero Valent Copper within the Matrix of Anion Exchangers via Green Chemical Reduction. *Polymers* **2020**, *12*, 2629. [CrossRef]
40. Ford, W.E. *Dana's Textbook of Mineralogy: With an Extended Treatise on Crystallography and Physical Mineralogy*, 4th ed.; CBS Publishers: New Delhi, India, 2006; 851p.
41. Ünaleroğlu, C.; Mert, Y.; Zümreoğlu-Karan, B. Synthesis and characterization of copper ascorbate. *Synth. React. Inorg. Met.-Org. Chem.* **2001**, *31*, 1531–1543. [CrossRef]
42. Stefanowicz, T.; Osinska, M.; Napieralska-Zagozda, S. Copper recovery by the cementation method. *Hydrometallurgy* **1997**, *47*, 69–90. [CrossRef]